NANO LETTERS

2006
Vol. 6, No. 11
2630−2636

Rapid and Sensitive Detection of Respiratory Virus Molecular Signatures Using a Silver Nanorod Array SERS Substrate

Saratchandra Shanmukh,[†] Les Jones,[§] Jeremy Driskell,[†] Yiping Zhao,[‡] Richard Dluhy,[†] and Ralph A. Tripp*[,§]

Department of Chemistry, Physics and Astronomy and Center for Disease Intervention, Department of Infectious Diseases, University of Georgia, Athens, Georgia 30602

Received July 19, 2006; Revised Manuscript Received September 12, 2006

ABSTRACT

A spectroscopic assay based on surface enhanced Raman scattering (SERS) using silver nanorod array substrates has been developed that allows for rapid detection of trace levels of viruses with a high degree of sensitivity and specificity. This novel SERS assay can detect spectral differences between viruses, viral strains, and viruses with gene deletions in biological media. The method provides rapid diagnostics for detection and characterization of viruses generating reproducible spectra without viral manipulation.

Introduction. Rapid and sensitive pathogen detection is central to human health care, required for proper therapeutic treatment, and required for prevention and control of pandemics or bioterrorism. The majority of existing viral detection assays employ antibody-based methods that include enzyme-linked immunosorbant assays (ELISA),[1] fluorescent antibody assays,[2] or serologic testing.[17] These methodologies lack the sensitivity and specificity required for low level virus detection, therefore more costly and laborious polymerase chain reaction (PCR) assays are often necessary to enhance virus detection.[8] Since these diagnostic methods are generally cumbersome and often have limited sensitivity, a variety of new virus detection methods, including microcantilevers,[9] evanescent wave biosensors,[4] immunosorbant electron microscopy,[31] and atomic force microscopy,[12] have been investigated to overcome these limitations. However, these new techniques are unable to discriminate between virus species with reasonable sample throughput, thus there is an unmet need for a rapid, reproducible, and sensitive means of detecting viruses that may inflict substantial burdens on human and animal health.

Raman spectroscopy has previously been used to characterize virus structure;[27] however, normal, un-enhanced Raman spectroscopy has an extremely small scattering cross section, which limits its use as a low level bioanalytical sensor. Surface-enhanced Raman spectroscopy (SERS) is a variation of Raman in which the incoming laser beam interacts with electrons in plasmon oscillations in metallic nanostructures to enhance, by orders of magnitude, the vibrational spectra of molecules adsorbed to the surface.[15] The morphology of the metallic nanostructures is a primary factor determining the magnitude of signal enhancement and sensitivity of detection.[25] Since SERS is useful for determining molecular structural information, and because SERS provides ultrasensitive detection limits including single molecule sensitivity,[11,29] it has been used to detect bacteria[21] and viruses using direct spectroscopic characterization[1] or reporter molecule sandwich assemblies. [5] However this remarkable analytical sensitivity has, for the most part, not translated into the development of practical in-situ diagnostic SERS probes.[15] This is due in large part to the difficulty in easily preparing robust, metal-coated substrates of the correct surface morphology that provide maximum SERS enhancements. We recently showed that a silver (Ag) nanorod SERS array fabricated using the oblique angle deposition (OAD) method acts as an extremely sensitive SERS substrate with enhancement factors of greater than 10^8.[3,30] The nanofabrication technique (OAD) offers a flexible, easy, and inexpensive method for fabrication of integrated nanoprobes for high sensitivity SERS applications. The SERS substrates produced by OAD have the advantages of large area, uniform, reproducibility. These novel substrates allow us to develop SERS-based biosensors rapidly, accurately, and cost-effectively to detect extremely low levels of viruses, thus bridging a critical need for a rapid, sensitive, and reliable

* Corresponding author.
[†] Department of Chemistry.
[‡] Department of Physics and Astronomy.
[§] Department of Infectious Diseases.

10.1021/nl061666f CCC: $33.50
Published on Web 09/30/2006

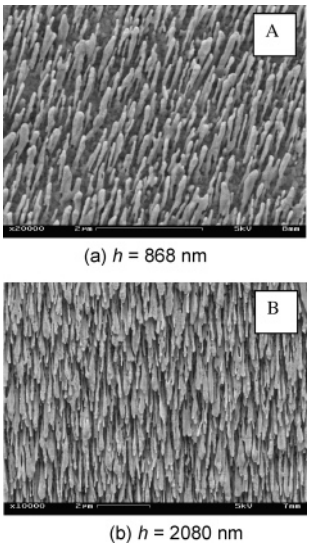

Figure 1. Representative scanning electron micrographs of the Ag nanorod arrays deposited with different lengths, (a) $h = 868$ nm and (b) $h = 2080$ nm. The typical SERS substrate used for virus detection is represented in (a) i.e. 870 nm.

means of diagnosing or detecting viruses that does not currently exist. In the study, we use the optimal Ag nanorod arrays generated by OAD and SERS to rapidly (30−50 s) detect in real-time human viruses in diminutive specimen volumes, and differentiate between respiratory viruses, virus strains, and viruses containing gene deletions without manipulating the virus.

Experimental Methods. *Substrates*. The SERS substrates were fabricated using a custom-designed electron beam/sputtering evaporation (E-beam) system (Torr International, New Windsor, NY), as previously described.[3] Briefly, in oblique angle deposition (OAD), the angle of depositing vapor and the surface normal of the substrate is set to be 86° where typically a base layer of 500 nm Ag thin film is deposited. With increasing deposition time, randomly distributed but aligned nanorod arrays develop on the substrate. Figure 1 shows two representative scanning electron microscope (SEM) images of Ag nanorod surfaces at length $h = 868$ nm and $h = 2080$ nm, respectively. The length of the nanorods increases monotonically as a function of deposition time, and the nanorods are tilted with respect to the normal of the substrate surface. The optimal SERS substrates observed in our previous experiments are shown in Figure 1a.[3,30] SEM images show the overall rod length of the nanorod substrates to be 868 nm ± 95 nm, while the diameter of the nanorods was 99 nm ± 29 nm. The density of the nanorods was calculated to be 13.3 ± 0.5 rods μm^{-2} with an average tilt angle of 71.3° ± 4.0°.

Viruses. The following human respiratory viruses were used in the analyses: respiratory syncytial virus (RSV) strain A2, RSV strain A/Long, RSV strain B1, recombinant wild type RSV strain A2 (6340), 6340 with a deletion of the G gene (ΔG), rhinovirus type 4/strain 16/60 (rhino), adenovirus type 6/tonsil strain 99 (Ad), a CXCR4-tropic strain of human immunodeficiency virus (HIV), and influenza (flu) virus strains A/HKx31, A/WSN/33, and A/PR/8/34. RSV, Ad and rhino viruses were propagated using Vero cells maintained in Dulbecco's Modified Eagles Medium (DMEM; GIBCO BRL laboratories, Grand Island, NY) supplemented with 2% heat-inactivated (56 °C) FBS (Hyclone Laboratories, Salt Lake City, UT). Upon detectable cytopathic effect, RSV, Ad and Rhino viruses were harvested in serum-free DMEM followed by two freeze−thaws (−70 °C/4 °C), after which the contents were collected and centrifuged at 4000 *g* for 15 min at 4 °C. The virus titers were similar and ranged between 5×10^6 and 1×10^7 PFU/mL, determined by immunostaining plaque assay as previously described.[26] The control for these studies was uninfected Vero cell lysate cleared of cell debris by centrifugation (4000 *g*, 15 min, 4 °C). Influenza strains were propagated in embryonated chicken eggs and virus titers determined by hemagglutination assay using chicken red blood cells. The influenza virus titers ranged between 10^7 and 10^8 EID_{50}. The control for these studies was naïve allantoic fluid. HIV was propagated by infecting human white blood cells previously stimulated with phytohemmaglutinin (Sigma) as described,[14] and titers assayed by ID50 to determine the number of infectious particles per mL. As necessary, viruses were inactivated by 4% paraformaldehyde treatment at room temperature for 3 hours.

Virus Purification. RSV purification was done on a sucrose cushion to allow comparison of spectral bands in the SERS spectrum of RSV infected cell lysate to virus alone. The purification was done as previously described with slight modifications.[7,13] Briefly, RSV-infected cell lysate was layered onto a 77% sucrose solution in MHN buffer (0.1 M magnesium sulfate, 0.15 M sodium chloride, 0.05 M HEPES) and centrifuged at 27 000 × g for 1.5 h at 4 °C. The interphase was collected, diluted with 2 volumes of MHN buffer, and layered onto a step gradient of 77% sucrose in MHN buffer and 33% sucrose in MHN buffer and centrifuged at 100 000 × g for 1 h at 4 °C. The interphase on the top layer containing purified RSV was collected and dialyzed against PBS. The concentrations of the purified virus samples were $\sim 5 \times 10^8$ PFU/mL.

Surface Enhanced Raman Spectroscopy. SERS spectra were acquired using a near-IR confocal Raman microscope system (Hololab Series 5000, Kaiser Optical Systems, Inc., Ann Arbor, MI). A fiber-optic interfaced 785 nm near-IR diode laser (Invictus, Kaiser Optical) was used as the laser source, and the spectrograph was a Kaiser Optical Holospec *f*/1.8-NIR equipped with a LN_2-cooled CCD camera (1024EHRB, Princeton Instruments, Trenton, NJ). The laser power at the sample varied between 10 and 15 mW with spectral collection times in the range 30−50 s. A 0.5−1.0 μL sample of intact virus was applied to the array Ag nanorod substrate and allowed to bind for 1 h at room temperature prior to spectrum acquisition. SERS spectra were collected from multiple spots across the substrate and from multiple substrates.

Experimental Results. To determine the capacity of SERS to distinguish different RNA viruses, the baseline corrected enhanced Raman spectra of adenovirus (Ad), rhinovirus (rhino), and human immunodeficiency virus (HIV) was determined (Figure 2). The SERS Ad spectrum (Figure 1a)

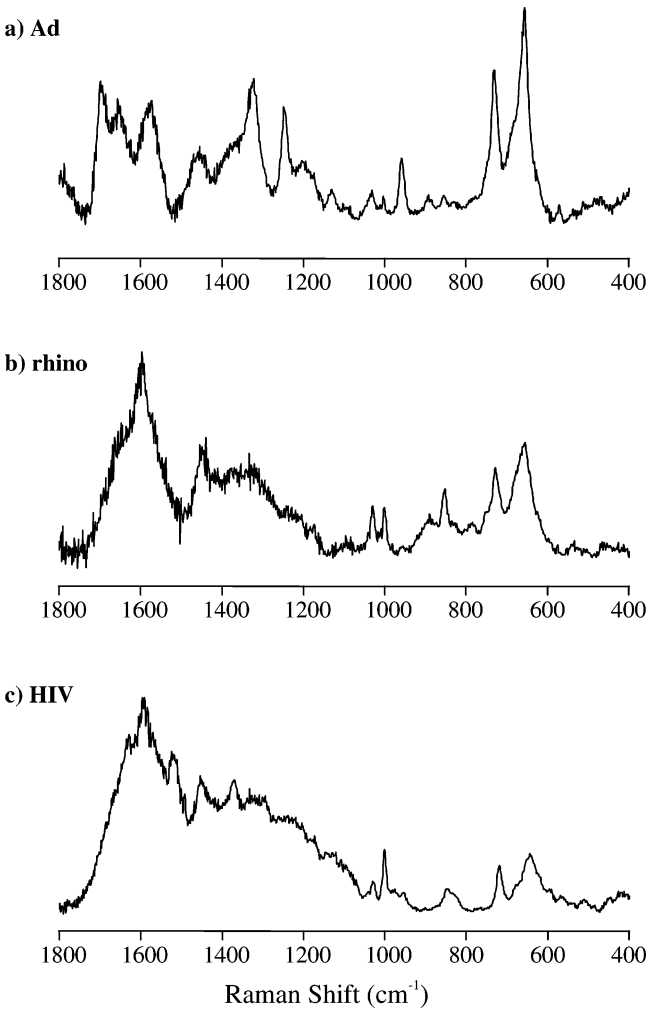

Figure 2. SERS spectra of (a) adenovirus (Ad), (b) rhinovirus (rhino), (c) and HIV viruses. Raman bands can be assigned to chemical constituents such as nucleic acid bases, amino acids, and proteins for all the spectra. The most prominent spectral features observed in the spectra are at 654 cm^{-1}, 730 cm^{-1}, 1247 cm^{-1}, and 1326 cm^{-1} corresponding to guanine, the adenine ring vibration, thymine, and adenine respectively. The Raman bands between 1580 cm^{-1} and 1700 cm^{-1} can be attributed to carbonyl groups on the amino acid side chains and the Amide I vibration while the spectral region near 1000 cm^{-1} has bands due top phenylalanine (1001 cm^{-1} and 1030 cm^{-1}).

is characterized by strong bands due to nucleic acid bases at 650 cm^{-1} (guanine), 731 cm^{-1} (adenine), 1325 cm^{-1} (adenine), and 1248 cm^{-1} (guanine).[18] The 650 cm^{-1} band may also have contributions due to Tyr.[19] The Raman lines at 1003 cm^{-1} and 1033 cm^{-1} have been assigned to the symmetric ring breathing mode and the in-plane C−H bending mode of Phe, respectively,[20] while the bands at 1457 cm^{-1}, 1576 cm^{-1}, and 1655 cm^{-1} can be attributed to the CH_2 deformation mode of proteins, the carboxylate stretching vibration ($\nu_a COO^-$) of Trp and the amide I vibration of the peptide groups, respectively.[20] A notable characteristic of the SERS Ad spectrum is the relative intensity of the bands associated with the nucleic acids indicating direct binding to the Ag substrate. The strong band at 731 cm^{-1} has been assigned to denatured DNA caused by its interaction with the Ag SERS substrate.[10]

In the SERS spectrum for rhino (Figure 2b), the major Raman bands are present at 656 cm^{-1} (guanine), 729 cm^{-1} (adenine), 853 cm^{-1} (Tyr), 1002 cm^{-1} and 1030 cm^{-1} (Phe), 1448 cm^{-1} (CH_2 deformation), and 1597 cm^{-1} ($\nu_a COO^-$ Trp). Comparison of this spectrum with the SERS Ad spectrum shows a clear shift in the frequency of the guanine band. Other differences that distinguish the SERS spectrum of rhino from Ad are the relative intensities of the nucleic acid bands compared to the other bands in the spectrum, and the absence of strong nucleic acid bands at higher wave number positions.

For the SERS HIV spectrum (Figure 2c), the Raman bands at 643 cm^{-1}, 719 cm^{-1}, 848 cm^{-1}, 1002 cm^{-1}, 1371 cm^{-1}, 1454 cm^{-1}, and 1523 cm^{-1} can be assigned to guanine, adenine, Tyr, Phe, the $\nu_s COO^-$ stretch of Trp, CH_2 deformation band and the $\nu_a COO^-$ of Trp, respectively. Notable differences in the SERS HIV spectra compared to Ad or rhino are the shifted spectral positions of the guanine band (643 cm^{-1}) and the adenine band (719 cm^{-1}), and the presence of a band at 1523 cm^{-1} in the HIV spectrum that is absent in the spectra of the other two viruses. Based on the differences in the SERS spectra, it was possible to distinguish between the three viruses investigated in this study. This result highlights the potential of SERS as a tool to rapidly detect and identify different viral pathogens in trace amounts in diminutive specimen volumes in real-time.

To show that SERS virus detection is not confounded by the biological media supporting the virus, we compared the SERS spectra of uninfected Vero cell lysate (VCL), RSV-infected Vero cell lysate (RSV), and purified RSV (Figure 3). The results show that major Raman bands can be assigned to different constituents of the cell lysate and the virus, such as nucleic acids, proteins, protein secondary structures, and amino acid bonds present in the side chains or backbone. It should be noted that blank Ag nanorod SERS substrates produced using OAD methods normally have background spectral contributions that have previously been attributed to carbonaceous material adsorbing onto the substrate during the fabrication of the SERS substrate and storage in ambient conditions.[24] Such background signals are commonly encountered in SERS. However, these bands were found to remain unchanged throughout the studies and exposure to laser radiation did not affect their position or intensities. The bands present in the figures that may have underlying contributions from substrate background signals have been identified with asterisks.

Virus spectra collected from multiple spots on the SERS substrate were similar except for minor differences in relative band widths and intensities. In the SERS spectrum of purified RSV (Figure 3c), the bands at 527 cm^{-1} and 546 cm^{-1} can be assigned to a disulfide stretching mode.[6,22] The strong band at 837 cm^{-1} may have some contribution from the background signal of the substrate; however, the band position corresponds to a Tyr. The main feature of this spectrum is a strong band at 1044 cm^{-1} that has been assigned to the C−N stretching vibration in previous SERS studies.[1,23] Since RSV has spike-like glycoprotein projections on the membrane envelope comprising two major glycopro-

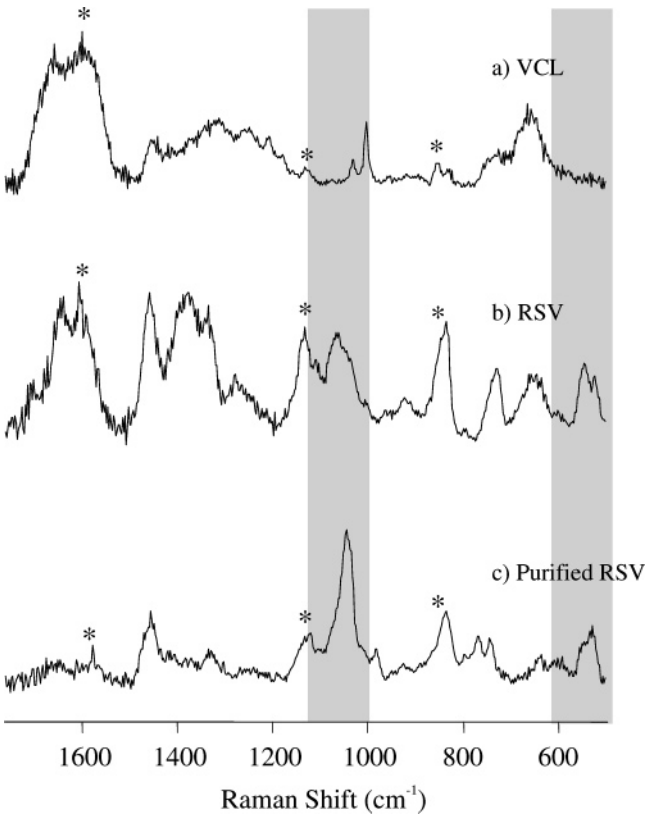

Figure 3. SERS spectra of (a) uninfected Vero cell lysate (VCL), (b) RSV-infected cell lysate (RSV), and (c) purified RSV. Spectral bands can be observed at 1066 cm^{-1} (C−N stretch), 835 cm^{-1} (tyrosine), and a doublet at 545 cm^{-1} and 523 cm^{-1} (S−S) that are present in the SERS spectrum of the RSV infected cell lysate sample but not in the spectrum of the uninfected cell lysate. The bands in the spectra that may have some contribution from the background signal of the SERS substrate are identified by asterisks.

teins, i.e., F and G glycoprotein, it is likely that the virus binds to the SERS substrate through an amino group giving rise to a strong band due to the C−N stretching mode.[20] The Raman band at 1456 cm^{-1} can be assigned to the CH_2 deformation vibration arising from the proteins or the lipids in the membrane. In the case of the SERS spectrum of the uninfected VCL, the bands at 658 cm^{-1} and 730 cm^{-1} can be assigned to the nucleic acids guanine and adenine, respectively,[18] while the other observed Raman bands in the spectrum can be assigned to amino acids and Amide I and III vibrations.[20] The SERS spectrum of the RSV-infected cell lysate shows several bands that are also observed in the VCL spectrum and can be attributed to the constituents of cell debris. However, strong bands can be observed at 1066 cm^{-1} (C−N stretch), 835 cm^{-1} (Tyr), and a doublet at 545 cm^{-1} and 523 cm^{-1} (disulfide stretch) that are present in the SERS spectrum of the RSV-infected cell lysate, but not in the spectrum of VCL. The appearance of these bands clearly indicates the presence of RSV in the cell lysate. The difference in the frequency of the C−N stretching mode between the purified RSV and RSV-infected cell lysate is most likely due to components in the VCL. The results suggest SERS can readily detect a virus, e.g., RSV in a variety of biological media.

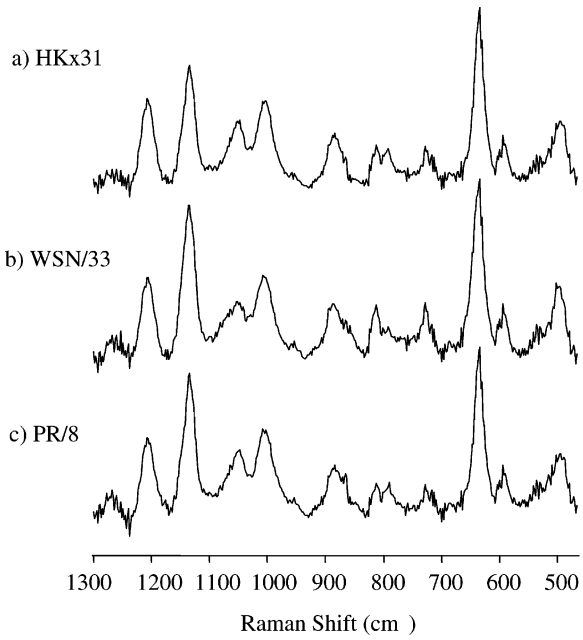

Figure 4. SERS spectra of (a) A/HKx31 influenza virus (HKx31), (b) A/WSN/33 influenza virus (WSN/33), and (c) A/PR/8/34 (PR/8). Spectra collected from multiple spots for individual strains were summed and normalized to the intensity of the most intense band.

Since SERS could detect and distinguish between different viral pathogens (Figure 2), it was important to determine if different viral strains from a single pathogen could be distinguished. To address this possibility, influenza virus (flu) A strain viruses A/HKx31, A/WSN/33, and A/PR/8/34 were analyzed by SERS. Influenza is an enveloped virus with two major glycoproteins on its surface, i.e., hemagglutinin and neuraminidase which are used to differentiate influenza subtypes. SERS analysis of the three strains of flu A and the corresponding baseline corrected spectra (1300−500 cm^{-1}) are shown in Figure 4. The main bands in the spectra appear at 1206 cm^{-1} (Tyr), 1130 cm^{-1} ν(C−C), 1047 cm^{-1} ν(C−N), 1003 cm^{-1} (Phe), 885 cm^{-1} (Gly), 635 cm^{-1} (Tyr), and 592 cm^{-1} (Gly) can be assigned to amino acid, protein, and nucleic acid molecules. The band at 812 cm^{-1} has been assigned to the phosphate backbone stretch of the RNA on previous bulk Raman studies on viruses.[28] The results suggest that the spectra of the three viruses are similar; however, there are differences in the relative intensities of the peaks in the spectra. This could be due to a difference in the nature of binding of the surface proteins of this particular virus on the SERS substrate surface. Thus, SERS detection of flu strain spectra is sufficiently different to allow identification of individual strains in a complex mixture. This effect is most evident in the spectral regions between 900−700 cm^{-1}, which show intensity differences as well as frequency shifts in the spectra for the three flu strains.

The small variations in the individual SERS spectra of a particular viral strain arise mostly due to slight heterogeneity in substrate morphology and differences in orientation of the components of the viruses on the substrate. To be able to distinguish strains based on their SERS spectra, it is important that the variations in the spectra of individual strains are not greater than the differences between strains.

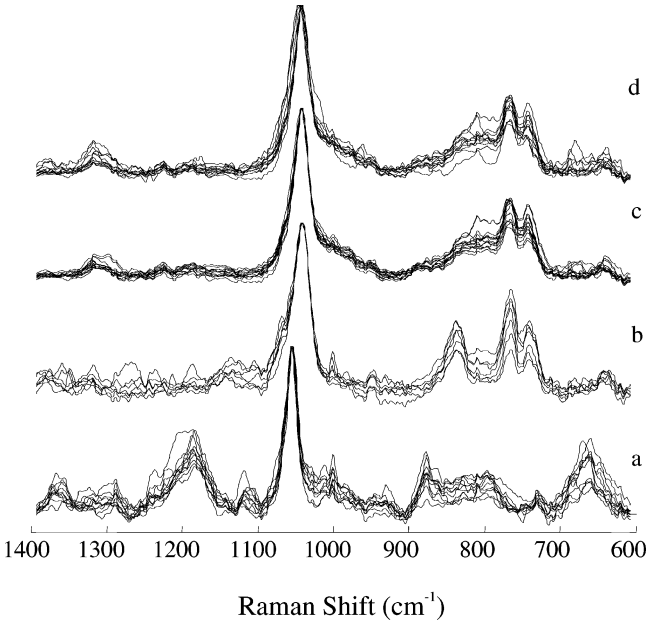

Figure 5. SERS spectra of the RSV strains (a) strain A/Long (A/Long), (b) strain B1 (B1), (c), strain A2 with a G gene deletion (ΔG), and (d) strain A2 (A2), collected from several spots on multiple substrates and normalized to the peak intensity of the most intense band (1045 cm^{-1}) and overlaid to illustrate the reproducibility on the Ag nanorod substrate.

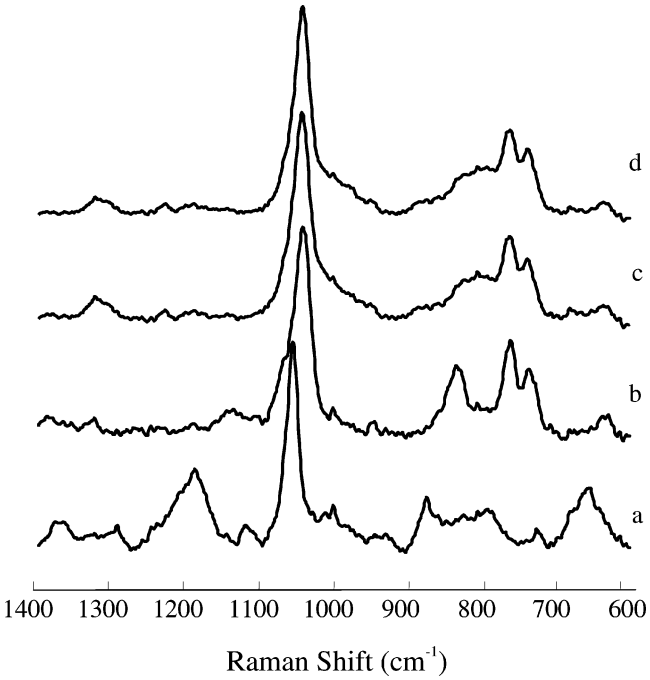

Figure 6. Summed SERS spectra of the individual RSV strains (a) strain A/Long (A/Long), (b) strain B1 (B1), (c), strain A2 with a G gene deletion (ΔG), and (d) strain A2 (A2) to show the differences between strains after compensating for substrate heterogeneity. The spectra were baseline corrected and smoothed for a clearer view of the spectral differences.

The spectra of individual viral strains obtained on the silver nanorod substrates used in this investigation have a high degree of reproducibility. SERS spectra of the RSV strains, collected from separate spots on the substrate and from three different substrates, were normalized with respect to the most intense band in each spectrum and are displayed in Figure 5. The RSV strains examined were RSV A strains A/Long, A2, ΔG, and the RSV B strain, B1. The region from 600−1400 cm^{-1} is displayed since most of the differences between the spectra are observed here. Looking at the overlaid spectra of each individual strain it is apparent that there is a high degree of spot-to-spot and substrate-to-substrate reproducibility. At the same time, from the stacked spectra it is obvious that there are distinct spectral differences between the RSV viral strains. To clearly show that the variability in the spectra of individual strains do not prevent the ability to discriminate between strains, the spectra of each strain shown in Figure 5 were summed up and normalized with respect to the most intense band and are overlaid in Figure 6. By adding spectra from multiple spots, the variation arising due to substrate surface heterogeneity and molecular orientation can be compensated to enable a "variable-independent" comparison. Based on the findings for influenza virus strains (Figure 4), and the observation that primary Raman bands arise due to surface proteins and nucleic acids, minor but notable differences were expected in the Raman spectra for RSV strains. The SERS spectrum of A/Long (Figure 6a) differed from the other RSV spectra in band frequency of the main band in the spectrum that is due to the C−N stretch occurring at 1055 cm^{-1} compared to 1042−1045 cm^{-1} for the other RSV strains and bands unique to A/Long observed at 877 cm^{-1} and 663 cm^{-1}. It is likely that the different spectrum observed for A/Long virus relates to the different nucleic acid composition and the proteins present on the viral envelope. There were also differences in the SERS spectra between RSV A strains and the B1 strain. The differences that distinguished the SERS A strain spectra from the SERS B strain spectrum include the relative intensities of the nucleic acid bands compared to the other bands in the spectrum.

To investigate the sensitivity and analytical utility of the SERS methodology, several dilutions of the RSV ΔG virus were analyzed. RSV ΔG virus solutions of different titers were prepared by dilution with deionized water and 0.3 μL of the solutions were applied to the Ag nanorod array substrates and allowed to dry and five spectra were collected from different locations on the substrate for each concentration. Figure 7 plots the peak area of the main band at 1045 cm^{-1} against the RSV ΔG virus concentration. The concentrations of the diluted solutions were calculated from the volume of water used for the dilutions. As is evident from the plot, as the concentration of the viral solution is decreased, the SERS intensity decreases linearly from 10^3 PFU/mL over 2 orders of magnitude. However, the intensity begins to plateau or even decrease at concentrations above 10^3 PFU/mL. This behavior is not uncommon and similar findings of decreasing signal with increasing concentration have been reported for SERS substrates with an adsorbate coverage ≥0.01 monolayer.[16] Although at this stage minimal effort was placed on determining the lowest detectable titer, values as low as 100 PFU/mL were readily detectable.

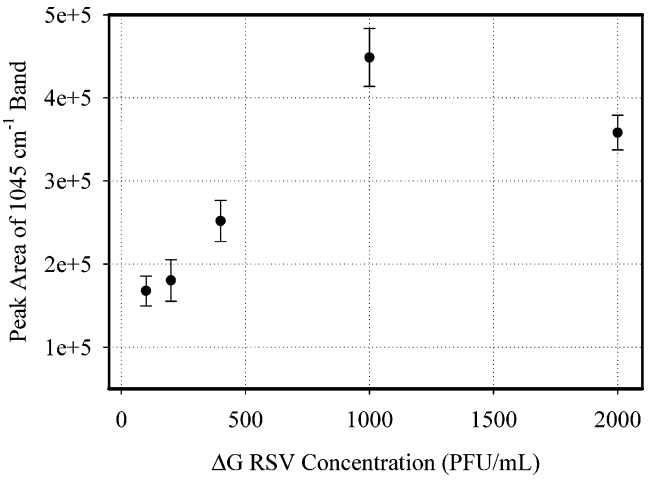

Figure 7. The SERS calibration curve for ΔG RSV constructed with the peak area for the C−N stretching band at 1045 cm^{-1}. Each data point represents the average signal from five different locations in the sample area. The standard deviation in the measurements is represented by the error bars.

Discussion. There is a critical need for a rapid and reliable means of detecting very low levels of viruses which may cause disease in both human and animals and pose a significant threat as an agent of bioterrorism. Current viral diagnostic methods are cumbersome, time-consuming, and have limited sensitivity. The emergence of nanotechnology holds the promise of developing biosensors that will allow for the direct, rapid, and sensitive detection of infectious agents. Among the biosensing methods being explored in virus research, SERS has gained particular interest over the past few years due to its ability to simultaneously provide extremely low detection limits as well as structural and quantitative information about the analytes.[17,25] Recent development of nanofabrication techniques employing oblique angle deposition allow for the production of Ag nanorod substrates that exhibit extremely high ($\sim 10^8$) SERS enhancement factors,[3,30] thus providing novel and powerful biosensing methods.

The SERS spectra associated with the nanostructured metal substrate and analyte of interest provides rapid detailed fingerprint information about the molecular composition of the adsorbed biomaterial in a nondestructive manner. The technology and methodology to acquire and interpret biological SERS spectra is currently available and relatively easily applied. The results of these studies show that the SERS spectra of viruses can be used to rapidly distinguish between viruses and virus strains, thus serving as a rapid and reproducible means to molecularly fingerprint viruses. These results also suggest that is possible to use SERS to collect the spectra of various viruses and virus strains to develop a reference library of vibrational Raman fingerprints that can be used to rapidly and accurately identify viruses in very small (0.5−1.0 μL) volumes.

Conclusions. Compared to previous studies relying on bulk Raman analysis of viruses, the SERS studies shown here represent a dramatic biotechnological advancement allowing for more rapid observation of Raman spectra of extremely small amounts and concentrations of analyte, particularly since the spectra can be obtained with greatly reduced data accumulation times and incident laser powers. The speed, specificity and relative ease of implementation of the SERS technique make it a very important alternative to current viral diagnostic tools and methodologies, and offers new virus detection means that are central to human health care.

Acknowledgment. SS and RAD are supported by the NIH grant EB001956. Y.P.Z. acknowledges the support from the NSF (ECS-0304340). R.T. acknowledges the support from the Georgia Research Alliance. The authors thank Stephen Chaney for preparation of the substrates and Drs. Stephen Mark Tompkins, T. Honeycutt Hodge and Rene Gomez Alvarez for preparation of some of the viruses.

References

(1) Bao, P.-D.; Huang, T.-Q.; Liu, X.-M.; Wu, T.-Q. *J. Raman Spectrosc.* **2001**, *32*, 227−230.
(2) Barenfanger, J.; Drake, N.; Leon, N.; Mueller, T.; Troutt, T. *J. Clin. Microbiol.* **2000**, *38*, 2824−2828.
(3) Chaney, S. B.; Shanmukh, S.; Zhao, Y.-P.; Dluhy, R. A. *Appl. Phys. Lett.* **2005**, *87*, 31908−31910.
(4) Donaldson, K. A.; Kramer, M. F.; Lim, D. V. *Biosens. Bioelectron.* **2004**, *20*, 322−327.
(5) Driskell, J. D.; Kwarta, K. M.; Lipert, R. J.; Porter, M. D.; Neill, J. D.; Ridpath, J. F. *Anal. Chem.* **2005**, *77*, 6147−6154.
(6) Edwards, H. G. M.; Hunt, D. E.; Sibley, M. G. *Spectrochim. Acta Part A***1998**, *54*, 745−757.
(7) Fernie, B. F.; Gerin, J. L. *Virology* **1980**, *106*,141−144.
(8) Henkel, J. H.; Aberle, S. W.; Kundi, M.; Popow-Kraupp, T. *J. Med. Virol.* **1997**, *53*, 366−371.
(9) Ilic, B.; Yang, Y.; Craighead, H. G. *Appl. Phys. Lett.* **2004**, *85*, 2604−2606.
(10) Kneipp, K.; Flemming, J. *J. Mol. Struct.* **1986**, *145*, 173−179.
(11) Kneipp, K.; Wang, Y.; Kneipp, H.; Perelman, L. T.; Itzkan, I.; Dasari, R.; Feld, M. S. *Phys. Rev. Lett.* **1997**, *78*, 1667−1670.
(12) Kuznetsov, Y. G.; Daijogo, S.; Zhou, J.; Semler, B. L.; McPherson, A. *J. Mol. Biol.* **2005**, *347*, 41−52.
(13) Mbiguino, A.; Menezes, J. *J. Virol. Methods* **1991**, *31*, 161−170.
(14) McDougal, J. S.; Cort, S. P.; Kennedy, M. S.; Cabridilla, C. D.; Feorino, P. M.; Francis, D. P.; Hicks, D.; Kalyanaraman, V. S.; Martin, L. S. *J. Immunol. Methods* **1985**, *76*,171−183.
(15) Moskovits, M. *J. Raman Spectrosc.* **2005**, *36*, 485−496.
(16) Norrod, K. L.; Sudnik, L. M.; Rousell, D.; Rowlen, K. L. *Appl. Spectrosc.* **1997**, *51*, 994−1001.
(17) O'Shea, M. K.; Ryan, M. A. K.; Hawksworth, A. W.; Alsip, B. J.; Gray, G. C. *Clin. Infect. Dis.* **2005**, *41*, 311−317.
(18) Otto, C.; Vandentweel, T. J. J.; Demul, F. F. M.; Greve, J. *J. Raman Spectrosc.* **1986**, *17*, 289−298.
(19) Peticolas, W. L.; Patapoff, T. W.; Thomas, G. A.; Postlewait, J.; Powell, J. W. *J. Raman Spectrosc.* **1996**, *27*, 571−578.
(20) Podstawka, E.; Ozaki, Y.; Proniewicz, L. M. *Appl. Spectrosc.* **2004**, *58*, 570−580.
(21) Premasiri, W. R.; Moir, D. T.; Klempner, M. S.; Krieger, N.; Jones, G., II; Ziegler, L. D. *J. Phys. Chem. B* **2005**, *109*, 312−320.
(22) Qian, W. L.; Krimm, S. *J. Raman Spectrosc.* **1992**, *23*, 517−521.
(23) Stewart, S.; Fredericks, P. M. *Spectrochim. Acta Part A***1999**, *55*, 1615−1640.
(24) Taylor, C. E.; Garvey, S. D.; Pemberton, J. E. *Anal. Chem.* **1996**, *68*, 2401−2408.
(25) Tian, Z. Q.; Ren, B.; Wu, D. Y. *J. Phys. Chem. B* **2002**, *106*, 9463−9483.
(26) Tripp, R. A.; Moore, D.; Jones, L.; Sullender, W.; Winter, J.; Anderson, L. J. *J. Virol.* **1999**, *73*, 7099−7107.

(27) Tuma, R.; Thomas, G. J., Jr. Raman spectroscopy of viruses. In Chalmers, J. M., Griffiths, P. R., Eds.; *Handbook of Vibrational Spectroscopy*; John Wiley & Sons: Chichester, 2002; Vol. 5.
(28) Verduin, B. J. M.; Prescott, B.; Thomas, G. J. *Biochemistry* **1984**, *23*, 4301−4308.
(29) Xu, H.; Bjerneld, J.; Käll, M.; Börjesson, L. *Phys. Rev. Lett.* **1999**, *83*, 4357−4360.
(30) Zhao, Y.-P.; Chaney, S. B.; Shanmukh, S.; Dluhy, R. A. *J. Phys. Chem. B* **2006**, *110*, 3135−3157.
(31) Zheng, Y. Z.; Hyatt, A.; Wang, L. F.; Eaton, B. T.; Greenfield, P. F.; Reid, S. *J. Virol. Methods* **1999**, *80*, 1−9.

NL061666F